



## DETERMINATION OF THIN-FILM DEBONDING PARAMETERS FROM TELEPHONE-CORD MEASUREMENTS

G. GIOIA<sup>1</sup> and M. ORTIZ<sup>2\*</sup>

<sup>1</sup>Department of Aerospace Engineering and Mechanics, University of Minnesota, Minneapolis, MN 55455 and <sup>2</sup>Graduate Aeronautical Laboratories, California Institute of Technology, Pasadena, CA 91125, U.S.A.

(Received 26 February 1997; accepted 26 June 1997)

**Abstract**—Methods are put forward for the determination of the fracture energy and kinetic coefficient of thin film/substrate interfaces from measurements performed on telephone cord blisters. This work is based on a previously proposed model for the characterization of debonding features in compressed thin films. The advantages of the proposed methods stem from the following facts concerning telephone cord blisters: (i) they are spontaneous debonding features, and therefore more amenable than artificially contrived features to yield realistic debonding parameters; (ii) they are very commonly observed in compressed thin films; (iii) as revealed by our model, their boundaries are characterized by a constant fracture mode mixity, and (iv) the driving force for debonding equals the fracture energy everywhere on their boundaries.

### 1. INTRODUCTION

Thin films deposited on substrates are being employed in numerous engineering applications. Among these applications we can instance wear-resistant coatings in machining tools; protective, insulating, and diffusive barriers in integrated circuits; protective, reflective, and reflexive layers in optical lenses; and thermal barriers in engine components. (For a recent review see [1]). In many of these applications the film/substrate system is prone to fail by film debonding, a process which is frequently driven by highly compressive in-plane stresses in the film. The interface adhesion is therefore a quantity of utmost importance to assess the structural integrity of these systems. (Here we use the term “adhesion” without implying strict interfacial failure; for a discussion of this and other relevant terms see [2]).

Many of the tests advanced so far yield qualitative measures of adhesion which are useful for comparison purposes only. Those most widely known are the Peel test [3]; the Scratch test [4]; the Pull test [5]; and the Laser Spallation test [6]. All of them are available in many different versions; more recent references include [7–10]. (For extensive reviews see [11,12]). Even when the fracture-mechanics conditions attendant to debonding can be calculated for these tests, those conditions are usually complex and involve non-uniform mode mixity; as a result, the fracture energy is difficult to estimate. These

tests are easily performed, however, which makes them very useful for certain applications. A good example is afforded by the oldest test available, which was advanced by Strong in 1935 under the name of “Scotch Tape test” [3]. Strong used his method in the manufacture of astronomical mirrors, as a pass/no pass test to ascertain the quality of the surface cleaning which precedes the deposition of a reflective aluminium film on glass. The method is still employed for similar purposes.

Although well-characterized procedures to measure fracture energies of film/substrate interfaces remain scant [12], a few tests have been designed capable of yielding reliable, quantitative measurements. We can instance the blister test of Bennett *et al.* [13] (a configuration first introduced by Hoffman and Geogoussis [14]); the indentation test of Evans and Hutchinson [15]; and the double cantilever beam test of Cannon *et al.* [16]. More recent versions of these tests include [17–19]. Other studies have endeavored to obtain values of fracture energy from measurements performed on spontaneous debonding features. This has been deemed the most rational approach, because it dwells on the expected modes of failure [12]. Thus, Argon *et al.*, Gupta and Hutchinson *et al.* [20–23] computed debonding fracture energies by performing coupled buckling/fracture analyses of equiaxed blisters of a type sometimes observed in compressed thin films. In a similar vein, Matuda *et al.* [24] computed fracture energies from experimental observations of webs of blisters (Section II.C). Other researchers have focused their attention on the tele-

\*To whom correspondence should be addressed.

phone cord morphology, a form of debonding which is ubiquitous in compressed thin films ([1] Section II.C). For instance, Gille and Rau [25], and Ogawa *et al.* [26] computed values of fracture energies by applying, as an approximation, formulae for straight blisters to telephone-cord measurements.

In Section 2 of this paper we resort to a previously proposed theory ([1]; see also [27]) to advance a method for the determination of fracture energies from measurements performed on telephone cord blisters. The theory is based on nonconvex analysis, matched asymptotic expansions, and interfacial fracture mechanics. One remarkable prediction of the theory concerns the mode mixity on the debonding front, which turns out to be uniform in all cases. An excellent agreement with the observed geometry of telephone cords was obtained for a special class of *critical* solutions, wherein the driving force equals the fracture energy everywhere on the debonding front ([1] Section IV.C). Together with the noted pervasiveness of telephone cords in compressed thin films, these results point to the telephone cord as an ideal spontaneous debonding mode on which to base a method for fracture energy determination.

The proposed method requires the measurement of the film thickness, the stress in the film prior to debonding, and the wavelength—or, alternatively, the width—of the telephone cord; the film/substrate interface fracture energy corresponding to the dominant mode mixity follows from substitution of these values in a simple explicit formula, equation (8). We illustrate the method by applying it to pertinent experimental data from the literature, and briefly discuss the results.

A second aspect of import to the mechanical assessment of thin film/substrate systems concerns the kinetics of film debonding. Whenever the driving force  $\mathcal{G}$  associated with the debonding front exceeds the fracture energy  $\mathcal{G}_c$ , further debonding is expected to occur. The net available driving force  $\mathcal{G} - \mathcal{G}_c$  may then be thought as imparting the debonding front a normal velocity  $V_n$ . Considerations of work conjugacy suggest that a kinetic relation of the form  $V_n = f(\mathcal{G} - \mathcal{G}_c)$  must rule this process, subject to the restrictions imposed by the second law [28]. This class of kinetic relations has been extensively treated within the theory of phase transitions [28]. In the context of dynamically growing cracks, these relations are often interpreted as crack-tip “equations of motion” [29], and have been investigated experimentally for a variety of bimaterial systems [30–32]. For the quasistatic type of growth often observed in thin-film blisters, by contrast, there is a paucity of experimental data to guide the formulation of kinetic relations (see [26, 33] for notable exceptions).

In Section 3 of this paper, we adopt a kinetic relation which is linear in the product of  $\mathcal{G} - \mathcal{G}_c$  and a

factor  $1/B$ , where  $B$  is the fracture kinetic coefficient. We then consider the feasibility of determining values of  $B$  from measurements performed on telephone cord blisters. These blisters are known to grow at the tip, a process which has been superbly documented by Ogawa *et al.* [26], and pointed out by other authors [23, 34–36]. Based on the theory developed in [1], we obtain solutions for the morphology of growing telephone cord tips. In these solutions the ratio  $\tilde{L}$  between the length and width of the tip is a function of a nondimensional parameter  $\Omega$ . The definition of  $\Omega$  involves both  $B$  and the time required for the growth of the cord in one wavelength, see Fig. 5. Figure 5 readily leads to a method for the determination of the kinetic coefficient  $B$  in terms of a simple formula, equation (15). We demonstrate the method by applying it to the experimental data of [26].

## 2. FRACTURE ENERGY

In [1], we advanced a model capable of characterizing the telephone cord morphology. For the details of the model we refer the reader to the original publication; here, we shall only review the principal assumptions in a brief manner.

The theory is based on the observation that the bending energy of the thin film is a singular perturbation of the membrane energy. This immediately suggests a matched asymptotic expansion, whereby the fundamental structure of the solution is dictated by the minimization of the membrane energy (the so-called *outer solution*), the bending energy being confined to narrow *bending boundary layers* located along the lines of slope discontinuity of the outer solution. An essential difficulty with this approach follows from the nonconvexity of the membrane energy functional, which makes the outer solution nonunique. In [1] Section III.D.3, we have argued, however, that the preferred outer solution may be determined as the upper envelope of all cones of characteristic slope  $k$  supported on the domain of the blister. The characteristic slope is given by  $k = \sqrt{2(1 + \nu)\epsilon^*}$ , where  $\epsilon^*$  is the compressive (isotropic) eigenstrain in the thin film prior to debonding, and  $\nu$  is the Poisson ratio of the thin film.

An analysis of the bending layer located along the boundary  $\Gamma$  of the blister can be performed by introducing a few approximations. Thus, in [1] Section IV.B we assumed that the film deflections  $w(\eta, \xi)$  vary quadratically along an axis  $\eta$  normal to  $\Gamma$ , where  $\xi$  is a curvilinear coordinate measured along  $\Gamma$ . The bending layer so defined extends up to a *matching distance*  $\eta_m$  at which the slope  $w_\eta$  attains the characteristic value  $k$  of the outer solution. The matching distance represents the width of the bending layer, and is given by  $\eta_m(\xi) = k/\chi(\xi)$ , where we have defined  $\chi(\xi) \equiv w_{,\eta\eta}(0, \xi)$ . The energy  $W$  of the bending layer can then be computed for a boundary

of arbitrary morphology; an equation of equilibrium follows immediately as

$$\delta W_{\delta \chi} = \mathcal{E}(\chi, \chi', \chi'', \chi''', \chi^{iv}; \kappa, \kappa', \kappa'') = 0, \quad (1)$$

where  $\kappa(\xi)$  is the distribution of local boundary curvatures, and the derivatives are taken with respect to the curvilinear boundary coordinate  $\xi$ . The expression of  $\mathcal{E}$  is too cumbersome to reproduce here.

Now, the driving force for debonding is given in this theory by the following formula [1] Section IV.A),

$$\mathcal{G} = \frac{D}{2} \chi^2. \quad (2)$$

Here,  $D \equiv Eh^3/12(1-\nu^2)$  is the bending stiffness of the film, where  $E$  is the Young's modulus and  $h$  the thickness of the film. By introducing a parameter  $\chi_c$  the fracture energy  $\mathcal{G}_c$  can be conveniently expressed in the form

$$\mathcal{G}_c = \frac{D}{2} \chi_c^2. \quad (3)$$

In this theory the *phase angle*  $\psi$  characterising the fracture mode mixity is constant on the debonding front, and corresponds to  $\tan \psi = -\cot \omega$  ([1], p. 172) where  $\omega$  is a function of the elastic constants of film and substrate (more precisely, of the Dundurs parameters of the film/substrate system; see [37]). It follows that the fracture energy is constant on the debonding front.

Turning back our attention to the equation (1) of equilibrium of the bending boundary layer, we narrow the class of solutions sought to that of *critical debonding fronts*, i.e. to debonding fronts wherein  $\mathcal{G} = \mathcal{G}_c$  (and  $\chi = \chi_c$ ) for all  $\xi$ . Then, (1) simplifies to a second order ODE in the local curvature  $\kappa$ . Using the following nondimensional variables:

$$\bar{\kappa} \equiv \kappa h/k, \quad \text{and} \quad \bar{\xi} \equiv \xi k/h, \quad (4)$$

and the nondimensional parameter

$$\bar{\kappa}_c = \kappa_c h/k \equiv \chi_c h/k^2, \quad (5)$$

the simplified equation of equilibrium becomes

$$\begin{aligned} 5\bar{\kappa}''\bar{\kappa}\bar{\kappa}_c^3(\bar{\kappa}_c - \bar{\kappa}) & [\bar{\kappa}(-2\bar{\kappa}^2 + 9\bar{\kappa}\bar{\kappa}_c - 6\bar{\kappa}_c^2) \\ & - 6\bar{\kappa}_c(\bar{\kappa} - \bar{\kappa}_c)^2 \ln(1 - \bar{\kappa}/\bar{\kappa}_c)] \\ & + 10\bar{\kappa}'^2\bar{\kappa}_c^3[\bar{\kappa}(-3\bar{\kappa}^3 + 22\bar{\kappa}^2\bar{\kappa}_c - 30\bar{\kappa}\bar{\kappa}_c^2) \\ & + 12\bar{\kappa}_c^3 + 12\bar{\kappa}_c(\bar{\kappa}_c - \bar{\kappa})^3 \ln(1 - \bar{\kappa}/\bar{\kappa}_c)] \\ & + 2\bar{\kappa}^5(\bar{\kappa} - \bar{\kappa}_c)^2(5\bar{\kappa}^2 - 13\bar{\kappa}\bar{\kappa}_c + 8\bar{\kappa}_c^2 + 5\bar{\kappa}_c^4) \\ & - 20\bar{\kappa}^4\bar{\kappa}_c^4(\bar{\kappa} - \bar{\kappa}_c)^3 \ln(1 - \bar{\kappa}/\bar{\kappa}_c) = 0, \end{aligned} \quad (6)$$

where the derivatives are taken with respect to  $\bar{\xi}$ .

The logarithmic terms in (6) introduce the constraint  $\bar{\kappa} < \bar{\kappa}_c$  on the attainable values of curvature. Without loss of generality, we consider solutions for which  $\bar{\kappa}'(0) = 0$ , and  $\bar{\kappa}(0) = \bar{\kappa}_0 < \bar{\kappa}_c$ . Figure 1 shows the results obtained by

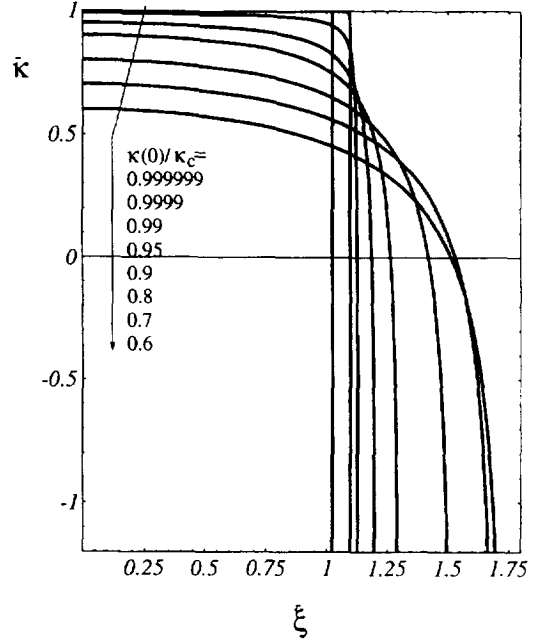


Fig. 1. trf: Family of solutions obtained for  $\nu_c = 1$ ,  $\bar{\kappa}'(0) = 0$ , and different values of  $\bar{\kappa}(0)/\bar{\kappa}_c < 1$ .

numerical integration with  $\bar{\kappa}_c = 1$ ; for all values of  $\bar{\kappa}_0$  a region of positive curvature is followed by a sharp dive into large negative curvatures, ending at a limit point  $\bar{\xi}_c$ , where the curvature becomes singular. When these solutions are reflected symmetrically with respect to  $\bar{\xi} = 0$ , and then extended periodically, the outcome is seen to describe the telephone cord morphology, with the characteristic pattern of broad intervals of positive curvature alternating with narrow sections of highly negative curvature or *cusps* [1], Section IV.C). The solution for  $\bar{\kappa}_0 \rightarrow \bar{\kappa}_c$  holds particular interest, because all the experimentally observed telephone cords which we analysed in [1], Section IV.D appear to correspond to this case. Here, arcs of length  $2/\bar{\kappa}_c$  and constant curvature  $\bar{\kappa}_c$  are punctuated by Dirac-deltas representative of sharp cusps (notice in Fig. 1 that the limit point for  $\bar{\kappa}_0 \rightarrow \bar{\kappa}_c$  is  $\bar{\xi}_c = 1/\bar{\kappa}_c$ , a conclusion which is valid for all values of  $\bar{\kappa}_c$ . This "universal geometry" is illustrated in Fig. 2, where we employ the notation  $\bar{\lambda} \equiv \lambda k/h$ ,  $\lambda$  being the wavelength of the telephone cord. Figure 2 furnishes then the equation

$$\bar{\lambda} = \frac{2}{\bar{\kappa}_c} \sin(1) = \frac{\lambda k}{h}. \quad (7)$$

where  $\sin(1) = \sin(34.38^\circ) \simeq 0.8415$ . By using (3) and (5), and taking into account that  $\sigma^* = Ec^*/(1-\nu)$ , where  $\sigma^*$  is the stress in the film before debonding, the following expression for the fracture energy can be readily derived:

$$\mathcal{G}_c = \frac{\sigma^* h^3}{3\bar{\lambda}^2} \sin^2(1). \quad (8)$$

In Table 1 we have compiled some of the available

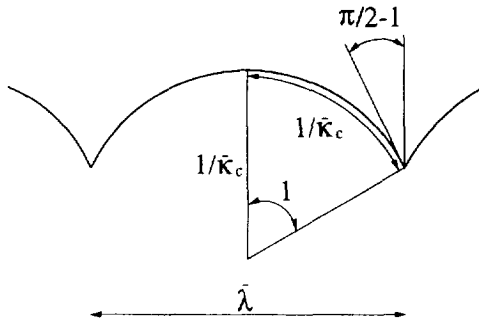


Fig. 2. "Universal geometry" of a telephone cord blister boundary ( $\kappa_0 \rightarrow \kappa_c$ ).

experimental data on telephone cord blisters, and the corresponding values of  $\mathcal{G}_c$  as determined by equation (8).

Both Ogawa *et al.* ([26] Mo/Glass system) and Gille and Rau ([25] C/Quartz system) computed values of fracture energy in their papers. Their values exceed by factors of 100–250, and 1000, respectively, those given in Table 1. (Daniels *et al.* [36], Iyer *et al.* [38], and Eymery and Boubeker [39] do not report fracture energies.) It is important to stress that these authors *computed* their values of fracture energy, to which effect they employed, as an approximation, formulae for straight cords. This amounts to imposing a geometric constraint, which results in larger values of energy release rate, and therefore in larger values of  $\mathcal{G}_c$ . In this respect, it is of interest to point out that Matuda *et al.* [24], in a study of a C/Quartz system similar to that of Gille and Rau, computed fracture energies by applying the same approximate model to a web of blisters, a configuration associated with larger energies than

the telephone cord: their estimated values of  $\mathcal{G}_c$  are one order of magnitude smaller than those of Gille and Rau.

The values of fracture energy in Table 1 must be interpreted with caution. They correspond to a specific phase angle  $\psi$  which is, according to our theory, characteristic of film/substrate interfaces in isotropically compressed thin films. They can readily be used to study debonding in such thin films. The extrapolation to different debonding conditions is not immediate. For example, in thin films with tensile eigenstrains, a different phase angle should be considered. However, the function  $\mathcal{G}_c(\psi)$  remains unexplored for the vast majority of film/substrate systems. In those few systems for which  $\mathcal{G}_c(\psi)$  has been characterized,  $\mathcal{G}_c$  appears to be highly sensitive to changes in  $\psi$  [37]. Furthermore, interface contamination may result in largely dissimilar values of fracture energy. For instance, thin film adhesion in the Mo/glass system (such as that tested by Ogawa *et al.*) is known to be very strongly dependent on subtle changes in environmental conditions (V. Gupta, private communication, 1997). The same appears to be true for a Cu/glass system studied by Cannon *et al.* [16], and perhaps for numerous other systems. Also, due to the effects of plasticity or damage certain debonding conditions may lead to highly nonlinear fracture, with vast effects on the apparent fracture energy [22]. For example, in the peel test of metallic films the plastic deformation has been shown to account for most of the energy release rate [40]. Because of these reasons it is important to compute fracture energies under conditions akin to those expected for in-service debonding.

Table 1. Fracture energies computed with the proposed method from measurements on telephone cords extracted from the literature

Interface	Deposition	$h$ ( $\mu\text{m}$ )	$\lambda$ ( $\mu\text{m}$ )	$\sigma^*$ (GPa)	$\mathcal{G}_c$ ( $10^{-3}\text{N/m}$ )
Mo/glass [26]	IBS <sup>1</sup>	0.30	32 <sup>2</sup>	20.4	130
Mo/glass [26]	IBS	0.30	28.6 <sup>2</sup>	16.4	130
Mo/glass [26]	MS <sup>3</sup>	0.92	200 <sup>2</sup>	2.00	9.2
Mo/glass [26]	MS	0.93	202 <sup>2</sup>	2.22	10
Fe-Pt/Si/c <sup>3</sup> [36]	sputter	1.00	55 <sup>5</sup>	1.36	110
DLC/glass <sup>6</sup> [38]	CVD <sup>7</sup>	0.25	50 <sup>8</sup>	3.00	4.4
C/Quartz [25]	IBD 2 kV <sup>9</sup>	0.20	31.3	3–4	5.8 7.7
C/Quartz [25]	IBD 0.9 kV	0.20	37.0	4–6	5.5 8.3
C/Si [25]	IBD 2 kV	0.20	17.0	3–4	20–26
C/Si [25]	IBD 0.9 kV	0.20	33.3	4–6	6.8 10
b.c.c.SS/f.c.c.SS <sup>10</sup> [39]	IBS	0.80	57–71 <sup>11</sup>	1.3–2.1	31–78

<sup>1</sup>Ion beam sputtered.

<sup>2</sup>Authors report telephone cord width,  $1/\kappa_c$ .

<sup>3</sup>Magnetron sputtered.

<sup>4</sup>This is a multilayered film; a first 20 Å Fe layer was followed by 200 Å of Pt, and these by successive 35 Å polycrystalline layers of Fe and Pt, until the total thickness was completed. The method is applied to this system as an approximation only.

<sup>5</sup>Measured on Fig. 4(a). Local curvature distributions ("intrinsic" functions of the tips) for different values of the nondimensional parameter  $\Omega$ ; and (b) corresponding tip shapes, with the cusp on the right-hand side.

<sup>6</sup>Diamond-like carbon.

<sup>7</sup>Chemical vapor deposition.

<sup>8</sup>Measured on Fig. 4(a) of the original paper.

<sup>9</sup>Ion beam deposited with the indicated value of ion acceleration voltage.

<sup>10</sup>b.c.c. 304L Stainless Steel (ferromagnetic) on f.c.c. Stainless Steel.

<sup>11</sup>Measured on Fig. 2(b) of the original paper; the wavelength varies within the indicated range, possibly due to interfacial inhomogeneities



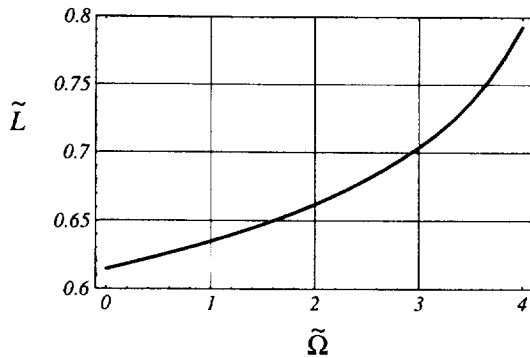


Fig. 5. Variation of the nondimensional tip length  $\tilde{L}$  as a function of  $\tilde{\Omega}$ .

*paribus* to faster tip growths—lead to longer tips. 55 shows the variation of the tip length  $\tilde{L} \equiv L\kappa_c$  (that is the maximum value of  $\tilde{x}_2$ ) with the parameter  $\tilde{\Omega}$ .

A method for the experimental determination of the fracture kinetic coefficient  $B$  is readily suggested by Fig. 5. Four measurements are required: the stress  $\sigma^*$ ; the width  $1/\kappa_c$  of the telephone cord; the length  $L$  of the tip; and the angular velocity  $\omega$ , which is conveniently expressed as  $\omega = 2/\tau$ , where  $\tau$  is the time required for the growth of the telephone cord by a wavelength  $\lambda$  (Fig. 2). Then,  $\Omega$  can be read from Fig. 5 as a function of  $\tilde{L} = L\kappa_c$ , and  $B$  computed using the following formula

$$B = \frac{1}{12} (h\kappa_c)^3 \tilde{\Omega} \sigma^* \tau. \quad (15)$$

An example of application of this method is afforded by the experimental results of Ogawa *et al.* [26]. These authors documented the growth of a telephone cord blister in a  $0.92 \mu\text{m}$ -thick Mo film which was magnetron-sputtered on a glass substrate. For this blister, Ogawa *et al.* reported the following data:  $E = 327 \text{ GPa}$ ,  $\nu = 0.3$ , and  $\epsilon^* = 0.005$ , corresponding to  $\sigma^* = 2.34 \text{ GPa}$ . From the microphotograph presented in Fig. 7 of Ogawa *et al.* (time = 512 s) we have measured  $1/\kappa_c = 90 \mu\text{m}$  and  $L = 60 \mu\text{m}$ , and verified that the tip length  $L$  is located off-center towards the side of the cusp, as predicted by our model (see Fig. 4(b)). It follows from these measurements that  $\tilde{L} = 0.67$ , and, from Fig. 5,  $\tilde{\Omega} = 2.2$ . Finally, from Fig. 8 of Ogawa *et al.* we have obtained  $\tau = 360 \text{ s}$ . Substituting these data in (15) we can compute the value  $B = 1.7 \cdot 10^{-5} \text{ N s/m}^2$  for the fracture kinetic coefficient of the Mo/glass interface.

#### 4. CONCLUSIONS

Telephone cord blisters are quite common in compressed thin films, where they occur spontaneously in many film/substrate systems. It therefore seems natural that several authors should have

advanced methods for the determination of fracture energy from measurements performed on telephone cord blisters. Unfortunately, lack of a better model has compelled these authors to base their methods on formulae for straight blisters, an approach which, although justifiable given the circumstances, remains far from satisfactory.

In devising the method proposed in this paper, we have resorted to a model which is remarkably successful at characterizing the telephone cord morphology in all its complexity. Somewhat surprisingly given the nature of the model—which involves nonconvex analysis, matched asymptotic expansions, and interface fracture mechanics—the formula for the fracture energy turns out to be quite simple: it is explicit, and involves quantities which can be readily measured on experimentally observed telephone cord blisters. For some film/substrate systems, the resulting values of fracture energy are substantially lower than those given by methods which interpret telephone cords as straight blisters. This appears to indicate that computed values of fracture energy are strongly affected by simplifications in blister geometry.

As for our method for kinetic coefficient determination, we have used the only complete data set available in the literature (Ogawa *et al.*) to compute what is, to the best of our knowledge, the first published value of kinetic coefficient for a film/substrate system.

#### REFERENCES

1. Gioia, G. and Ortiz, M., *Adv. Appl. Mech.*, 1997, **33**, 119.
2. Mittal, K. L., in *Adhesion Measurements of Thin Films, Thick Films, and Bulk Coatings*, ASTM STP 640, ed. K. L. Mittal. American Society for Testing and Materials, 1978, pp. 5–17.
3. Strong, J., *Rev. Sci. Instruments*, 1935, **6**, 97.
4. Heavens, O. S., *J. de Physique*, 1950, **11**, 355.
5. Belser, R. B. and Hicklin, W. H., *Rev. Sci. Instruments*, 1956, **27**, 293.
6. Vossen, J. L., in *Adhesion Measurement of Thin Films, Thick Films, and Bulk Coatings*, ASTM STP 640, ed. K. L. Mittal. American Society for Testing and Materials, 1978, pp. 122–133.
7. Kim, Y. H., Chang, Y. S., Chou, N. J. and Kim, J., *J. Vac. Sci. Tech.*, 1987, **5**, 2890.
8. Wu, T. W., *J. Mat. Res.*, 1991, **6**, 407.
9. Jacobsson, R. and Kruse, B., *Thin Solid Films*, 1973, **15**, 71.
10. Amaratunga, G. A. J. and Wellan, M. E., *J. Appl. Phys.*, 1990, **68**, 5140.
11. Mittal, K. L., *Electrocomponent Sci. and Tech.*, 1976, **3**, 21.
12. Alexopoulos, P. S. and O'Sullivan, T. C., *Ann. Rev. Mater. Sci.*, 1990, **20**, 391.
13. Bennett, S. J., Devries, K. L. and Williams, M. L., *Int. J. Fracture*, 1974, **10**, 33.
14. Hoffman, E. and Geogoussis, O., *J. Oil. Color. Chem. Assoc.*, 1959, **42**, 267.
15. Evans, A. G. and Hutchinson, J. W., *Int. J. Solids Struct.*, 1984, **20**, 455.
16. Cannon, R. M., Fisher, R. M. and Evans, A. G., *Mater. Res. Soc. Symp. Proc.*, 1986, **54**, 799.

17. Jensen, H. M. and Thouless, M. D., *Int. J. Solids Struct.*, 1993, **30**, 779.
18. Boer, M. P. and Gerberich, W. W., *Acta Mater.*, 1996, **44**, 3177.
19. Bagchi, A., Lucas, G. E. and Suo, Z., *J. Mater. Res.*, 1994, **9**, 1734.
20. Argon, A. S., Gupta, V., Landis, H. S. and Cornie, J. A., *J. Mater. Sci.*, 1989, **24**, 1207.
21. Argon, A. S., Gupta, V., Landis, H. S. and Cornie, J. A., *Mater. Sci. Engr.*, 1989, **A107**, 41.
22. Gupta, V., *Mater. Res. Soc. Bull.*, **39** 1991.
23. Hutchinson, J. W., Thouless, M. D. and Liniger, E. G., *Acta Metall. Mater.*, 1992, **40**, 295.
24. Matuda, N., Baba, S. and Kinbara, A., *Thin Solid Films*, 1981, **81**, 301.
25. Gille, G. and Rau, R., *Thin Solid Films*, 1984, **120**, 109.
26. Ogawa, K., Ohkoshi, T., Takeuchi, T., Mizoguchi, T. Masumoto, T., *Japanese J. Appl. Phys.*, 1986, **25**, 695.
27. Ortiz, M. and Gioia, G., *J. Mech. Phys. Solids*, 1994, **42**, 531.
28. Abeyaratne, R. and Knowles, J. K., *Arch. Rational Mech. Anal.*, 1991, **114**, 119.
29. Freund, L. B., *Dynamic Fracture Mechanics*. Cambridge University Press, New York, 1990.
30. Tippur, H. V. and Rosakis, A. J., *Exp. Mech.*, 1991, **31**, 243.
31. Liu, C., Lambros, J. and Rosakis, A. J., *J. Mech. Phys. Solids*, 1993, **41**, 1887.
32. Lambros, J. and Rosakis, A. J., *J. Mech. Phys. Solids*, 1995, **43**, 169.
33. Kinbara, A. and Baba, S., *J. Vac. Sci. Tech.*, 1991, **9**, 2494.
34. Nir, D., *Thin Solid Films*, 1984, **112**, 41.
35. Thouless, M. D., *J. Am. Ceram. Soc.*, 1993, **76**, 2936.
36. Daniels, B. J., Nix, W. D. and Clemens, B. M., in *Structure and Properties of Multilayered Thin Films*, *Mat. Res. Society Symposium Proceedings*, ed. T. O. Nguyen, B. M. Lairson, V. M. Clemens, S. C. Shin and H. Sato. Materials Research Society, 1995, Vol. 382, pp. 315–320.
37. Hutchinson, J. W. and Suo, Z., *Adv. Appl. Mech.*, 1991, **39**, 63.
38. Iyer, S. B., Harshavardhan, K. S. and Kumar, V., *Thin Solid Films*, 1995, **256**, 94.
39. Eymery, J. P. and Boubeker, B., *Materials Lett.*, 1994, **19**, 137.
40. Kim, K. S. and Aravas, N., *Int. J. Solids Struct.*, 1988, **24**, 417.